Journal of Biomechanics 190 (2025) 112885

Contents lists available at ScienceDirect

Journal of Biomechanics

journal homepage: www.elsevier.com/locate/jbiomech

# Effect of congruence variations on a musculoskeletal model considering humeral head displacements

Margaux Peixoto [a,*], Dan Soyeux [a], Patrice Tétreault [b], Mickaël Begon [c], Nicola Hagemeister [a]

[a] Laboratoire d'Innovation Ouverte, École de technologie Supérieure, Montréal, Canada
[b] Centre Hospitalier de l'Université de Montréal, Montréal, Canada
[c] Faculty of Medicine, University of Montreal, Montréal, Canada

ARTICLE INFO

*Keywords:*
Musculoskeletal shoulder model
Humeral head displacement
Rotator cuff muscles
Force-dependent kinematics
Congruency

ABSTRACT

The shoulder's large range of motion is due to the low congruency of the glenohumeral joint, whose stability relies mainly on rotator cuff muscle activity. The effect of joint congruence on shoulder biomechanics remains unclear. We used a sphere-on-sphere glenohumeral model combined with a Force-Dependent Kinematics algorithm to simulate muscle and joint forces while considering humeral head displacements. Our innovative simulations showed an increase in humeral head displacements and rotator cuff muscle forces when joint conformity decreased. Our model aligns with in vivo observations and highlights the importance of joint congruence on stability. It provides insights to improve our understanding of shoulder biomechanics.

## 1. Introduction

The shoulder's wide range of motion stems from scapula gliding on the thorax and the low congruency between the glenoid and humerus, with rotator cuff muscles providing active joint stabilization (Veeger and van der Helm, 2007). While in vivo studies report up to 12.4 mm superior humeral head migration during abduction (Dal Maso et al., 2014), most musculoskeletal models use ball-and-socket joints with three rotational degrees of freedom (DoF), underestimating rotator cuff muscle activation (Favre et al., 2009). To effectively address clinical questions, models must consider humeral head displacements (Bolsterlee et al., 2013) and joint instability metrics (Gerber et al., 2014).

Two methods enable humeral head displacements in musculoskeletal shoulder models: the sphere-on-sphere (SoS) model and force-dependent kinematics (FDK) algorithm. The SoS model mimics the anatomical glenohumeral displacements (El Habachi et al., 2015), by modeling the difference between glenoid ($32.2 \pm 7.6$ mm) and humeral head ($22.9 \pm 2.9$ mm) curvatures (McPherson et al., 1997). The ratio between humeral head and glenoid curvature radii—termed as the *conformity index*—ranges from $0.6 \pm 0.1$ for dry bones to $0.9 \pm 0.07$ with intact labrum and cartilage (Kelkar et al., 2001; Zumstein et al., 2014). It reflects the joint congruence which influences joint stability, with poor congruence correlating to greater humeral head displacement (Kelkar et al., 2001) and increased dislocation risk (Moroder et al., 2019; Peltz et al., 2015). The SoS model was implemented in a musculoskeletal model with only a passive contact element to prevent humeral head-glenoid penetration (Quental et al., 2016). Humeral head movement during abduction was minimal (<0.5 mm; close to a ball-and-socket joint) because they chose a high conformity (0.97). The effect of conformity on SoS model kinematics remains unstudied.

The FDK algorithm computes joint displacements iteratively to achieve static equilibrium (Andersen et al., 2017). Applications to shoulder models, both prosthetic (Sins et al., 2015; Strzelczak, 2021) and non-prosthetic (Aurbach et al., 2020; Menze et al., 2025), achieved $\sim 6$ mm displacements during $\leq 90°$ abduction. Both methods required passive stabilizing elements with challenging-to-define properties. Combining the kinematic constraint (El Habachi et al., 2015) with the FDK algorithm could eliminate this need. Given the limited research on congruence's effect on muscle recruitment (Karduna et al., 1996), this study aims to develop a shoulder model with physiological glenohumeral displacement and assess conformity index effects during over-the-shoulder abduction. We hypothesize that a SoS model with FDK-driven displacements can simulate in vivo humeral head

* Corresponding author at: Laboratoire d'Innovation Ouverte, 900, rue St-Denis, local R11.322, Montréal (Québec) H2X 0A9, Canada; 2188 av Valois, H1W 3M5 QC, Montréal, Canada.
*E-mail addresses:* margaux.peixoto.1@ens.etsmtl.ca (M. Peixoto), dan.soyeux.1@ens.etsmtl.ca (D. Soyeux), p.tetreault.md@gmail.com (P. Tétreault), mickael.begon@umontreal.ca (M. Begon), nicola.hagemeister@etsmtl.ca (N. Hagemeister).

https://doi.org/10.1016/j.jbiomech.2025.112885
Accepted 29 July 2025
Available online 5 August 2025

displacements and muscle activity patterns without passive elements.

## 2. Methods

### 2.1. Sphere-on-sphere glenohumeral musculoskeletal model

Our model relies on the AnyBody Managed Model Repository shoulder model (version 2.4.4) (Lund et al., 2023), replacing the ball-and-socket glenohumeral joint with a sphere-on-sphere joint (El Habachi et al., 2015). The scapular girdle uses a closed loop (thorax-clavicle-scapula-thorax), with two spheres representing the humeral head (smaller sphere; Fig. 1) and glenoid curvature (larger sphere). Radii of spheres vary to represent different plausible conformity indices of the glenohumeral joint. A kinematic constraint, a connecting rod of constant length between the sphere centers representing the glenoid and the humeral head (El Habachi et al., 2015), ensures the contact between the two bones. The glenohumeral joint has five DoFs: three in rotation, and two in translation driven by the FDK algorithm (Andersen et al., 2017). Displacements are iteratively optimized for quasi-static equilibrium within 0.1 N tolerance, without passive elements to favor stabilizing muscle activation. The model includes 104 Hill-type muscle fibers (Zajac, 1989), using unscaled Dutch Shoulder Group parameters (Van der Helm et al., 1992). Most fibers use via-point constraints, except for deltoid fibers (n = 12) using multi-ellipsoids (Strzelczak, 2021). The SoS model is available on GitHub: https://github.com/margauxpeixoto/GH_contact_spheres.

### 2.2. Simulation

Scapular plane abductions (10-130°), driven by humero-thoracic elevation angle, were simulated using the Anybody Modelling System (version 7.4.4). Scapulohumeral rhythm is implemented following de Groot and Brand (2001) equations. Joint torques were calculated using inverse dynamics, with muscle forces optimized to minimize *i)* the maximum of all the muscle forces and *ii)* the sum of the quadratic activations, a function that enhances co-activation (Rasmussen et al., 2001). The humeral head position is optimized iteratively thanks to the FDK algorithm (Andersen et al., 2017) by adding a force in the direction of the connecting rod to achieve a dynamic equilibrium. This force corresponds anatomically to the articular force of the glenoid on the humeral head. Glenohumeral joint compression and shear forces were then calculated. Instability was quantified using the instability ratio (Gerber et al., 2014): the ratio of shear forces to compression forces (Fshear/Fcompression). Humeral head displacements were measured in the glenoid reference frame, with positive values indicating posterior, superior, and medial directions.

### 2.3. Sensitivity study of the model to congruence variations

We assessed how joint congruence affects muscle and joint reaction forces using conformity indices of 0.6 (poorly congruent), 0.8, and 1.0 (perfect congruence/ball-and-socket), spanning literature-reported values (McPherson et al., 1997; Niu et al., 2023). After confirming that only the conformity index impacts outputs, we maintained a constant 20-mm glenoid radius (McPherson et al., 1997) and adjusted only the humeral head radius (Fig. 2, Appendix). The SoS implementation was verified by comparing r = 1 outputs with the original ball-and-socket model.

## 3. Results

### 3.1. Effect of congruence on humeral head displacement

As the conformity index decreased (0.8→0.6), humeral head displacements increased. In the posterior and medial directions, the displacements were less than 2 mm (Table 1). The largest displacements were observed in the superior direction. They increased in the initial phase of abduction, with the maximum displacement reached at 45° (3.24 and 8.7 mm for r = 0.8 and 0.6, respectively). Beyond 45° abduction, the displacement decreased to less than 1 mm at 130° abduction for all conformity indices.

### 3.2. Effect of congruence on muscle forces

A decrease in the conformity index affected the forces generated by the different parts of the deltoid and the rotator cuff muscles (especially the infraspinatus and subscapularis, little effect on the supraspinatus, and none on the teres minor; Fig. 3). Decreasing the conformity index led to an increase in the main stabilizing muscles of the joint: posterior deltoid, subscapularis, and infraspinatus forces. More specifically, the posterior deltoid played a greater role in compression after 45° of abduction. Reduced congruence increased the amplitude of the stabilizing forces generated by the infraspinatus and

**Table 1**
Effect of conformity index on humeral head displacement in three dimensions. Maximum displacements are shown in **bold.** The forces correspond to the total forces, i.e, both active and passive forces.

| Conformity indices | r = 0.8 | | | | r = 0.6 | | | |
|---|---|---|---|---|---|---|---|---|
| Abduction angle(°) | 10 | 45 | 90 | 130 | 10 | 45 | 90 | 130 |
| Posterior displacement (mm) | 0.2 | **0.4** | 0.4 | −0.2 | **1.3** | 1.3 | 1.1 | −0.6 |
| Superior displacement (mm) | 2.3 | **3.2** | 1.6 | −0.3 | 3.9 | **8.7** | 3.8 | −0.7 |
| Medial displacement (mm) | 0.1 | **0.3** | 0.0 | 0.2 | 0.4 | **1.0** | −0.8 | 0.4 |

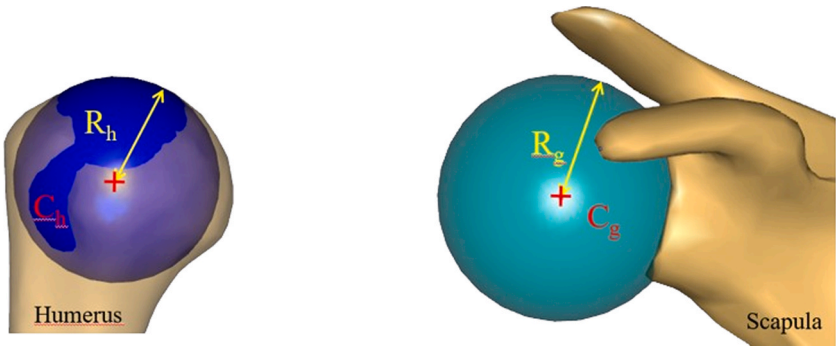


**Fig. 1.** Sphere-on-sphere glenohumeral joint with the humeral head represented by a blue sphere and the curvature of the glenoid by a green sphere. C and R represent the center of the sphere and the radius, respectively, with indices $_g$ and $_h$ for the glenoid cavity and humeral head, respectively.

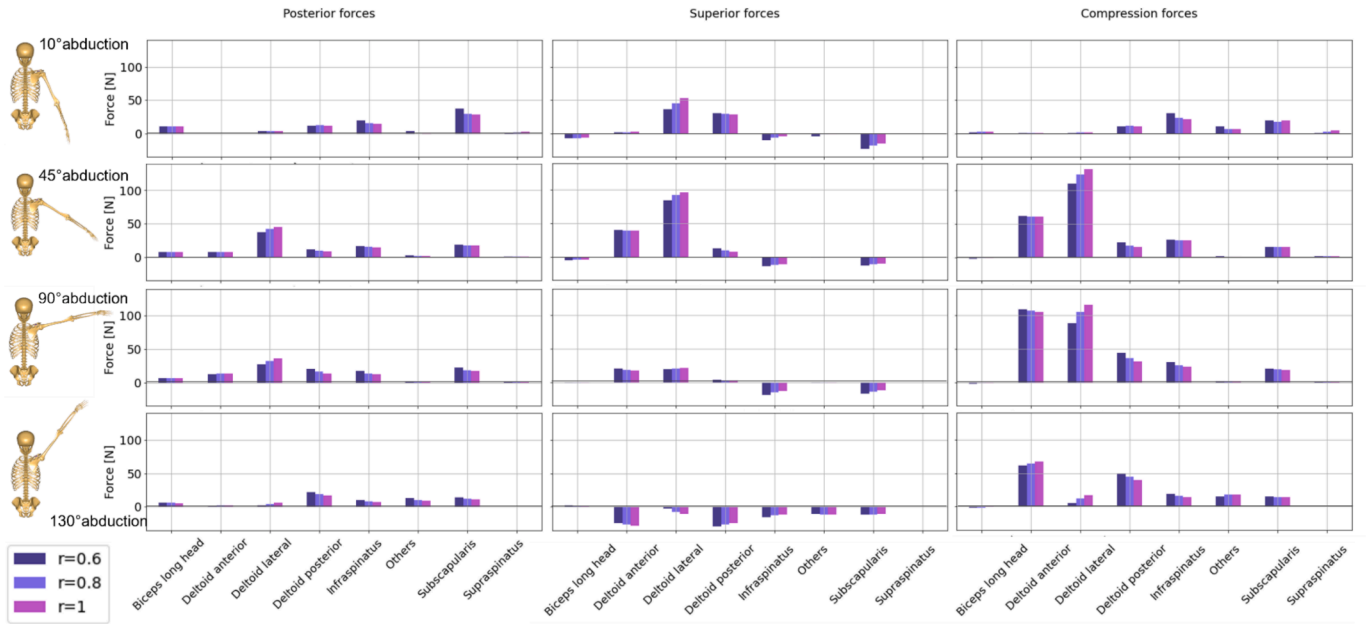


**Fig. 3.** Muscle forces during abduction at 10, 50, 90 and 130° for conformity indices of r = 1, r = 0.8 and r = 0.6.

subscapularis—specifically enhancing shear forces in the inferior and posterior directions and compressive forces—without altering their lines of action. The infraspinatus contributed primarily to compression and inferior shear force, while the subscapularis produced greater force in the posterior and inferior directions at the start of the movement (10° abduction).

On the contrary, increasing the conformity indices resulted in a decrease in the main abductor muscle forces, namely, the lateral deltoid and supraspinatus. The lateral deltoid produced the highest force (mostly compression but also superior shear forces) at 45° of abduction and the supraspinatus activated at the beginning of the abduction. The supraspinatus no longer generated force beyond 45° of abduction. The force generated by the teres minor, teres major, coracobrachialis, short head of biceps was not sensitive to congruence variations (5 N variations or less).

### 3.3. *Effect of congruence on the instability ratio*

The instability ratio was affected only in the first phase of the movement (below 45°), with the ratio increasing as the conformity index decreased (Fig. 4). The lower the conformity index, the higher the instability ratio. Above 45°, the instability ratio decreased for all conformity indices, reaching almost perfect stability at 130° of abduction.

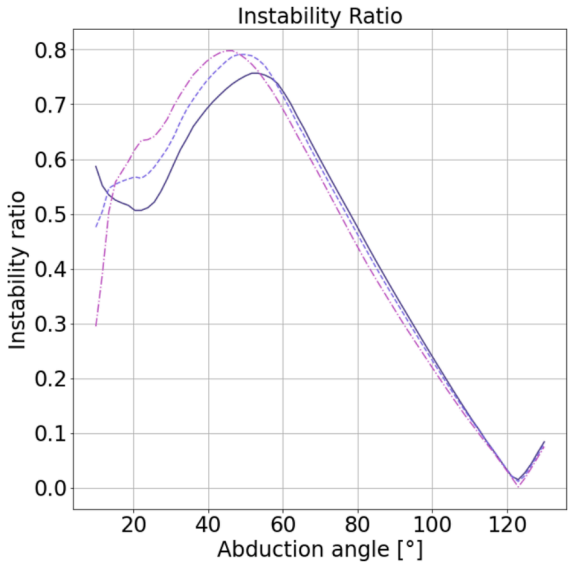


**Fig. 4.** Evolution of the instability ratio as a function of the abduction angle, for different conformity indices.

## 4. Discussion

We developed a shoulder model that combines sphere-on-sphere (SoS) and force-dependent kinematics (FDK) algorithms (SoS-FDK) to simulate humeral head displacement and investigate the impact of congruence (instability ratio) on shoulder muscle activation. Our innovative model was sensitive to variations in congruence, where decreased congruence led to increased instability, humeral head displacement, and greater activation of the cuff muscles.

In vivo, differences in acquisition methods and inter-subject variability result in a wide range of glenohumeral displacements. Moreover, the methods used to measure displacement vary across studies (Moissenet et al., 2024), complicating comparisons. Briefly, in-vivo displacements are mostly in the superior (up to 12.4 mm (Dal Maso et al., 2014)) and posterior (a few millimeters (Giphart et al., 2013)) directions. Peak displacement occurs in the middle of an arm abduction and decreases, with the humeral head centered at the end of abduction (Giphart et al., 2013). Our SoS-FDK model shows that, as congruence decreases, humeral head displacement increases—particularly in the superior and posterior directions—reproducing plausible kinematics with initial displacement followed by humeral head lowering. Because the objective function minimizes first and foremost the largest muscles force, the FDK algorithm optimizes the humeral position to improve the moment arm of the prime mover (i.e., lateral deltoid). After 45° of abduction, the FDK optimization lowers the humeral head to maximize the mechanical advantage of the lateral deltoid (Fig. 5, Appendix). This aligns with in vivo studies and the cadaveric study by (Kelkar et al., 2001). By reproducing these findings, our SoS-FDK model simulates more realistic kinematics than a ball-and-socket model.

Congruence has been identified as a key parameter in joint stability (Peltz et al., 2015). The lack of congruence between the humeral head and glenoid allows humeral head displacement, which is counteracted

by the activation of the cuff muscles (Veeger & van der Helm, 2007). However, muscle recruitment cannot be assessed in cadaveric studies, and in silico studies using a ball-and-socket model are inherently perfectly congruent. During the initial phase of movement, the lateral deltoid generates most muscle forces, pulling the humeral head upwards and explaining the superior migration of the humeral head. The supraspinatus in our model was activated, as reported by Escamilla et al. (2009) and Reed et al. (2013), but produced minimal force. This underactivation results from the quadratic term in the optimization function, which favors deltoid activation due to its larger moment arm. Reducing the weight of the quadratic term increases supraspinatus activation but introduces discontinuities (non-reported results). Future work should focus on optimizing via points and wrapping objects to enhance the supraspinatus moment arm.

From 45° abduction, and with reduced congruence, the infraspinatus, subscapularis, and posterior deltoid gradually produced more force, to lower the humeral head until it was centered at the end of the movement. Releasing DoFs in the SoS-FDK model allowed for a more physiological muscle activation pattern. It decreased the deltoid force, by improving its moment arm, while increasing the subscapularis and infraspinatus forces at mid-range abduction, as observed by Hawkes et al. (2019) and Escamilla et al. (2009).

Our SoS-FDK model simulated a more plausible representation of shoulder kinematics than ball-and-socket models, even though supraspinatus forces remained lower than expected. It allowed us to study the role of congruence in the activation of shoulder muscles responsible for joint stability. In our model, the instability ratio replicated the pattern seen by Gerber et al. (2014) on a shoulder simulator. However, the instability ratio in the SoS-FDK model was higher (the peak was between 0.7 and 0.8 depending on the conformity index vs. 0.4 for the simulator). We suggest that this higher ratio may be explained by the lower activation level of the supraspinatus during the initial phase of movement. We observed that the instability ratio was impacted only at the beginning of the movement, below 55° abduction. With greater abduction, increased force from the cuff muscles and posterior deltoid stabilized the joint, similar to a ball-and-socket model.

### *4.1. Limitations*

The biggest challenge for any model is validation. We compared the outputs of this model with results from other studies. Since muscle forces cannot be measured directly in vivo, we compared the muscle force range calculated by the SoS-FDK model with activation patterns estimated from EMG measurements, assuming a link between forces and activation, though this relationship remains debated (Liu et al., 1997; Woods & Bigland-Ritchie, 1983). The SoS-FDK model simplifies the glenoid representation as a sphere with uniform curvature radius, despite McPherson et al. (1997) reporting different conformity indices ($r = 0.72$ anteroposterior, $r = 0.63$ mediolateral) and Zumstein et al. (2014) finding plane-specific glenoid curvature radii. A sphere-on-ellipsoid model could improve this. The model also excludes soft tissues such as ligaments, cartilage, and labrum, which are crucial for joint stability (Halder et al., 2001; Lippitt et al., 1993). An exhaustive validation incorporating gold-standard kinematics, EMG data, and sensitivity analyses (e.g., muscle insertion locations; Chopp-Hurley et al., 2014) is required (Hicks et al., 2015). To quantitatively assess the SoS-FDK model predictions, we will compare predicted muscle activation patterns with intramuscular EMG data and humeral head translations with kinematics measured using intra-cortical pins (Dal Maso et al., 2014). Model parameters will be scaled to subject-specific anatomy to enable direct quantitative comparison with experimental data. Once validated, the SoS-FDK model will allow investigations of how humeral and scapular morphology influence joint stability, representing a significant improvement over ball-and-socket models that assume perfect congruence and fail to accurately represent the stabilizing role of muscles (Hill et al., 2008).

## 5. Conclusion

We developed a shoulder model that combined a sphere-on-sphere model with a force-dependent kinematics algorithm (SoS-FDK) to simulate humeral head translations without adding passive elements. Compared to the ball-and-socket model, the combination SoS and FDK model simulated plausible kinematics, muscle activation patterns, and resultant forces. Furthermore, this SoS-FDK model allowed us to study the influence of congruence on joint stability and shoulder muscle activation.

## CRediT authorship contribution statement

**Margaux Peixoto:** Writing – original draft, Visualization, Validation, Software, Project administration, Methodology, Investigation, Funding acquisition, Formal analysis, Data curation, Conceptualization. **Dan Soyeux:** Writing – review & editing, Visualization, Software, Methodology, Formal analysis. **Patrice Tétreault:** Writing – review & editing, Validation, Funding acquisition, Conceptualization. **Mickaël Begon:** Writing – review & editing, Validation, Supervision, Software, Methodology, Funding acquisition, Formal analysis, Conceptualization. **Nicola Hagemeister:** Writing – review & editing, Supervision, Resources, Project administration, Methodology, Funding acquisition, Formal analysis, Conceptualization.

## Declaration of competing interest

The authors declare that they have no known competing financial interests or personal relationships that could have appeared to influence the work reported in this paper.

## Acknowledgement

This research was funded by the Fonds de recherche du Québec - volet Technologie (B2X – 344407: https://doi.org/10.69777/344407). This finding support is not involved in the study design, in the collection, analysis and interpretation of data; in the writing of the manuscript; or in the decision to submit the manuscript for publication.

## Appendix

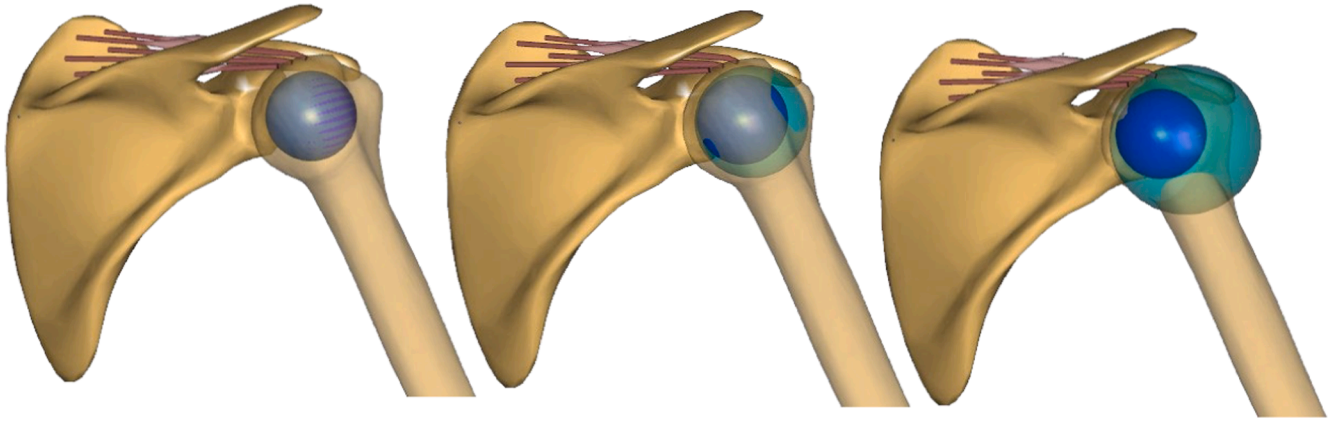

**Fig. 2.** Sphere-on-Sphere model represents congruences, from left to right: r = 1; r = 0.8 and r = 0.6. For clarity, only the supraspinatus is shown.

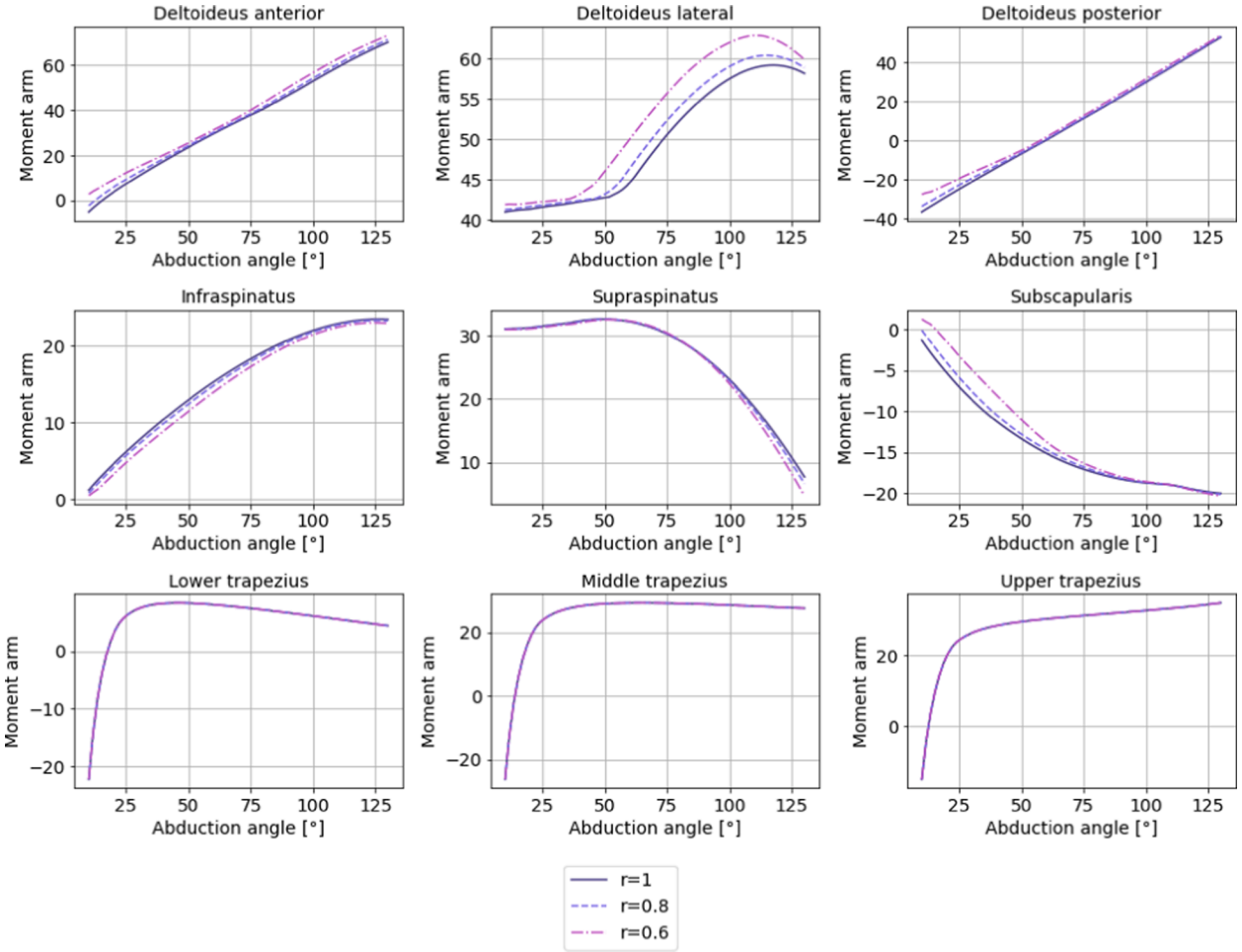


**Fig. 5.** The evolution of the moment arms of the main muscles according to congruence (r = 1 to r = 0.6) during scaption.

## References

Andersen, M., de Zee, M., Damsgaard, M., Nolte, D., Rasmussen, J., 2017. Introduction to Force-Dependent Kinematics : Theory and Application to Mandible Modeling. J. Biomech. Eng. 139 (9), 091001. https://doi.org/10.1115/1.4037100.

Aurbach, M., Spicka, J., Süß, F., Dendorfer, S., 2020. Evaluation of musculoskeletal modelling parameters of the shoulder complex during humeral abduction above 90°. J. Biomech. 106, 109817. https://doi.org/10.1016/j.jbiomech.2020.109817.

Bolsterlee, B., Veeger, D.H.E.J., Chadwick, E.K., 2013. Clinical applications of musculoskeletal modelling for the shoulder and upper limb. Med. Biol. Eng. Compu. 51 (9), 953–963. https://doi.org/10.1007/s11517-013-1099-5.

Chopp-Hurley, J.N., Langenderfer, J.E., Dickerson, C.R., 2014. Probabilistic Evaluation of Predicted Force Sensitivity to Muscle Attachment and Glenohumeral Stability uncertainty. Ann. Biomed. Eng. 42 (9), 1867–1879. https://doi.org/10.1007/s10439-014-1035-3.

Dal Maso, F., Raison, M., Lundberg, A., Arndt, A., Begon, M., 2014. Coupling between 3D displacements and rotations at the glenohumeral joint during dynamic tasks in healthy participants. Clin. Biomech. 29 (9), 1048–1055. https://doi.org/10.1016/j.clinbiomech.2014.08.006.

de Groot, J.H., Brand, R., 2001. A three-dimensional regression model of the shoulder rhythm. Clin. Biomech. 16 (9), 735–743. https://doi.org/10.1016/S0268-0033(01)00065-1.

El Habachi, A., Duprey, S., Cheze, L., Dumas, R., 2015. A parallel mechanism of the shoulder—Application to multi-body optimisation. Multibody Sys.Dyn. 33 (4), 439–451. https://doi.org/10.1007/s11044-014-9418-7.

Escamilla, R.F., Yamashiro, K., Paulos, L., Andrews, J.R., 2009. Shoulder Muscle activity and Function in Common Shoulder Rehabilitation Exercises. Sports Med. 39 (8), 663–685. https://doi.org/10.2165/00007256-200939080-00004.

Favre, P., Snedeker, J.G., Gerber, C., 2009. Numerical modelling of the shoulder for clinical applications. Philos. Trans. R. Soc. A Math. Phys. Eng. Sci. 367 (1895), 2095–2118. https://doi.org/10.1098/rsta.2008.0282.

Gerber, C., Snedeker, J.G., Baumgartner, D., Viehöfer, A.F., 2014. Supraspinatus tendon load during abduction is dependent on the size of the critical shoulder angle: a biomechanical analysis: CSA DEPENDENT SUPRASPINATUS LOAD. J. Orthop. Res. 32 (7), 952–957. https://doi.org/10.1002/jor.22621.

Giphart, J.E., Brunkhorst, J.P., Horn, N.H., Shelburne, K.B., Torry, M.R., Millett, P.J., 2013. Effect of Plane of arm Elevation on Glenohumeral Kinematics: a Normative Biplane Fluoroscopy Study. J. Bone Joint Surg. 95 (3), 238–245. https://doi.org/10.2106/JBJS.J.01875.

Halder, A.M., Zhao, K.D., O'Driscoll, S.W., Morrey, B.F., An, K.N., 2001. Dynamic contributions to superior shoulder stability. J. Orthop. Res. 19 (2), 206–212. https://doi.org/10.1016/S0736-0266(00)00028-0.

Hawkes, D.H., Khaiyat, O.A., Howard, A.J., Kemp, G.J., Frostick, S.P., 2019. Patterns of muscle coordination during dynamic glenohumeral joint elevation : an EMG study. PLoS One 14 (2), e0211800. https://doi.org/10.1371/journal.pone.0211800.

Hicks, J.L., Uchida, T.K., Seth, A., Rajagopal, A., Delp, S.L., 2015. Is my Model good Enough? best Practices for Verification and Validation of Musculoskeletal Models and Simulations of Movement. J. Biomech. Eng. 137 (2), 020905. https://doi.org/10.1115/1.4029304.

Hill, A.M., Bull, A.M.J., Wallace, A.L., Johnson, G.R., 2008. Qualitative and quantitative descriptions of glenohumeral motion. Gait Posture 27 (2), 177–188. https://doi.org/10.1016/j.gaitpost.2007.04.008.

Karduna, A.R., Williams, G.R., Iannotti, J.P., Williams, J.L., 1996. Kinematics of the glenohumeral joint : Influences of muscle forces, ligamentous constraints, and articular geometry. J. Orthop. Res. 14 (6), 986–993. https://doi.org/10.1002/jor.1100140620.

Kelkar, R., Wang, V.M., Flatow, E.L., Newton, P.M., Ateshian, G.A., Bigliani, L.U., Pawluk, R.J., Mow, V.C., 2001. Glenohumeral mechanics : a study of articular geometry, contact, and kinematics. J. Shoulder Elbow Surg. 10 (1), 73–84. https://doi.org/10.1067/mse.2001.111959.

Lippitt, S.B., Vanderhooft, J.E., Harris, S.L., Sidles, J.A., Harryman, D.T., Matsen, F.A., 1993. Glenohumeral Stability from Concavity-Compression : a Quantitative Analysis. J. Shoulder Elbow Surg. 2 (1), 27–35. https://doi.org/10.1016/s1058-2746(09)80134-1.

Liu, J., Hughes, R.E., Smutz, W.P., Niebur, G., Nan-An, K., 1997. Roles of deltoid and rotator cuff muscles in shoulder elevation. Clin. Biomech. (Bristol, Avon) 12 (1), 32–38. https://doi.org/10.1016/s0268-0033(96)00047-2.

Lund, M. E., Tørholm, S., Divyaksh S. Chander, & Menze, J. (2023). *The AnyBody Managed Model Repository (AMMR)* (Version 2.4.2) [Logiciel]. Zenodo. 10.5281/ZENODO.6809697.

McPherson, E.J., Friedman, R.J., An, Y.H., Chokesi, R., Dooley, R.L., 1997. Anthropometric study of normal glenohumeral relationships. J. Shoulder Elbow Surg. 6 (2), 105–112. https://doi.org/10.1016/S1058-2746(97)90030-6.

Menze, J., Croci, E., Andersen, M. S., Hess, H., Müller, A. M., Mündermann, A., & Gerber, K. (s. d.). *THE INFLUENCE OF MUSCULAR MODELING ON GLENOHUMERAL STABILITY IN A SHOULDER MODEL CONSIDERNG FORCE DEPENDENT KINEMATICS*.

Moissenet, F., Puchaud, P., Naaïm, A., Holzer, N., & Begon, M. (2024). *Spartacus-shoulder-kinematics-dataset/shoulder-kinematics congress* (Version 0.1.0) [Logiciel]. Zenodo. 10.5281/ZENODO.11455521.

Moroder, P., Damm, P., Wierer, G., Böhm, E., Minkus, M., Plachel, F., Märdian, S., Scheibel, M., Khatamirad, M., 2019. Challenging the Current Concept of critical Glenoid Bone loss in Shoulder Instability : does the size Measurement really tell it all? Am. J. Sports Med. 47 (3), 688–694. https://doi.org/10.1177/0363546518819102.

Niu, Z., Shen, X., Li, M., Fan, M., Zuo, J., Liu, T., 2023. Comparison of Glenohumeral Bone Morphology between patients with Versus without Anterior Shoulder Instability. Orthop. J. Sports Med. 11 (12), 23259671231217971. https://doi.org/10.1177/23259671231217971.

Peltz, C.D., Zauel, R., Ramo, N., Mehran, N., Moutzouros, V., Bey, M.J., 2015. Differences in glenohumeral joint morphology between patients with anterior shoulder instability and healthy, uninjured volunteers. J. Shoulder Elbow Surg. 24 (7), 1014–1020. https://doi.org/10.1016/j.jse.2015.03.024.

Quental, C., Folgado, J., Ambrósio, J., Monteiro, J., 2016. A new shoulder model with a biologically inspired glenohumeral joint. Med. Eng. Phys. 38 (9), 969–977. https://doi.org/10.1016/j.medengphy.2016.06.012.

Rasmussen, J., Damsgaard, M., Voigt, M., 2001. Muscle recruitment by the min/max criterion—A comparative numerical study. J. Biomech. 34 (3), 409–415. https://doi.org/10.1016/S0021-9290(00)00191-3.

Reed, D., Cathers, I., Halaki, M., Ginn, K., 2013. Does supraspinatus initiate shoulder abduction? J. Electromyogr. Kinesiol. 23 (2), 425–429. https://doi.org/10.1016/j.jelekin.2012.11.008.

Sins, L., Tétreault, P., Hagemeister, N., Nuño, N., 2015. Adaptation of the AnyBody™ Musculoskeletal Shoulder Model to the Nonconforming Total Shoulder Arthroplasty Context. J. Biomech. Eng. 137 (10), 101006. https://doi.org/10.1115/1.4031330.

Strzelczak, M. (2021). Development of a shoulder musculoskeletal model to assess the impact of scapular morphology on glenohumeral biomechanics. École de Technologie Supérieure.

Van der Helm, F.C.T., Veeger, H.E.J., Pronk, G.M., Van der Woude, L.H.V., Rozendal, R. H., 1992. Geometry parameters for musculoskeletal modelling of the shoulder system. J. Biomech. 25 (2), 129–144. https://doi.org/10.1016/0021-9290(92)90270-B.

Veeger, H.E.J., van der Helm, F.C.T., 2007. Shoulder function : the perfect compromise between mobility and stability. J. Biomech. 40 (10), 2119–2129. https://doi.org/10.1016/j.jbiomech.2006.10.016.

Woods, J.J., Bigland-Ritchie, B., 1983. Linear and non-linear surface EMG/force relationships in human muscles. an anatomical/functional argument for the existence of both. Am. J. Phys. Med. 62 (6), 287–299.

Zajac, F.E., 1989. Muscle and tendon : Properties, models, scaling, and application to biomechanics and motor control. Crit. Rev. Biomed. Eng. 17 (4), 359–411.

Zumstein, V., Kraljević, M., Hoechel, S., Conzen, A., Nowakowski, A.M., Müller-Gerbl, M., 2014. The glenohumeral joint - a mismatching system? a morphological analysis of the cartilaginous and osseous curvature of the humeral head and the glenoid cavity. J. Orthop. Surg. Res. 9 (1), 34. https://doi.org/10.1186/1749-799X-9-34.